Cytotherapy 000 (2023) 1–12

Contents lists available at ScienceDirect

CYTOTHERAPY

journal homepage: www.isct-cytotherapy.org

Full-length article

Stromal cell therapy

A robust and standardized method to isolate and expand mesenchymal stromal cells from human umbilical cord

Pia Todtenhaupt[1,2], Laura A. Franken[1], Sophie G. Groene[1,2], Marcella van Hoolwerff[1], Lotte E. van der Meeren[3,4], Jeanine M.M. van Klink[2], Arno A.W. Roest[5], Christiaan de Bruin[6], Yolande F.M. Ramos[1], Monique C. Haak[7], Enrico Lopriore[2], Bastiaan T. Heijmans[1], Melissa van Pel[8,9,*,**]

[1] *Molecular Epidemiology, Department of Biomedical Data Sciences, Leiden University Medical Center, Leiden, The Netherlands*
[2] *Neonatology, Willem-Alexander Children's Hospital, Department of Pediatrics, Leiden University Medical Center, Leiden, The Netherlands*
[3] *Department of Pathology, Leiden University Medical Center, Leiden, The Netherlands*
[4] *Department of Pathology, Erasmus Medical Center, Leiden, The Netherlands*
[5] *Pediatric Cardiology, Willem-Alexander Children's Hospital, Department of Pediatrics, Leiden University Medical Center, Leiden, The Netherlands*
[6] *Pediatric Endocrinology, Willem-Alexander Children's Hospital, Department of Pediatrics, Leiden University Medical Center, Leiden, The Netherlands*
[7] *Fetal Medicine, Department of Obstetrics, Leiden University Medical Center, Leiden, The Netherlands*
[8] *NecstGen, Leiden, The Netherlands*
[9] *Department of Internal Medicine, Leiden University Medical Center, Leiden, The Netherlands*

ARTICLE INFO

Article History:
Received 20 January 2023
Accepted 14 July 2023
Available online xxx

Key Words:
differentiation
mesenchymal stromal cells
platelet lysate
protocol standardization
umbilical cord

ABSTRACT

Background aims: Human umbilical cord–derived mesenchymal stromal cells (hUC-MSCs) are increasingly used in research and therapy. To obtain hUC-MSCs, a diversity of isolation and expansion methods are applied. Here, we report on a robust and standardized method for hUC-MSC isolation and expansion.
Methods: Using 90 hUC donors, we compared and optimized critical variables during each phase of the multi-step procedure involving UC collection, processing, MSC isolation, expansion and characterization. Furthermore, we assessed the effect of donor-to-donor variability regarding UC morphology and donor attributes on hUC-MSC characteristics.
Results: We demonstrated robustness of our method across 90 UC donors at each step of the procedure. With our method, UCs can be collected up to 6 h after birth, and UC-processing can be initiated up to 48 h after collection without impacting on hUC-MSC characteristics. The removal of blood vessels before explant cultures improved hUC-MSC purity. Expansion in Minimum essential medium α supplemented with human platelet lysate increased reproducibility of the expansion rate and MSC characteristics as compared with Dulbecco's Modified Eagle's Medium supplemented with fetal bovine serum. The isolated hUC-MSCs showed a purity of ~98.9%, a viability of >97% and a high proliferative capacity. Trilineage differentiation capacity of hUC-MSCs was reduced as compared with bone marrow-derived MSCs. Functional assays indicated that the hUC-MSCs were able to inhibit T-cell proliferation demonstrating their immune-modulatory capacity.
Conclusions: We present a robust and standardized method to isolate and expand hUC-MSCs, minimizing technical variability and thereby lay a foundation to advance reliability and comparability of results obtained from different donors and different studies.

Introduction

Isolation and expansion of primary cells from tissues often results in heterogeneous cell populations that may differ widely per culture due to the absence of standardized protocols and large donor-to-donor differences. To allow comparability between cells obtained from different donors within and between study cohorts and to

* Correspondence: Melissa van Pel, PhD, NecstGen, Sylviusweg 62, 2333 BE Leiden, The Netherlands.
** Department of Internal Medicine, Leiden University Medical Center, Albinusdreef 2, P.O. Box 9600, 2300 RC Leiden, The Netherlands.
E-mail address: m.van_pel@necstgen.com (M. van Pel).

https://doi.org/10.1016/j.jcyt.2023.07.004

generate reproducible results, standardized methods for cell isolation and expansion are key. Human umbilical cord–derived mesenchymal stromal cells (hUC-MSCs) are a cell type that is increasingly used as a therapeutic agent and research model [1–5]. Standardized methods for hUC-MSC isolation and expansion are currently lacking, impacting on comparability and reproducibility of results obtained in study cohorts.

MSCs are multipotent stromal precursor cells originating from the embryonic mesoderm [6,7]. They can be isolated from a variety of different adult and birth-associated tissues, such as bone marrow, adipose tissue, umbilical cord (UC), placenta, amnion and chorion [2,8,9]. As the isolation from birth-associated tissues poses less ethical concerns due to the non-invasive collection procedures, their use as a source for MSC, especially UC, has increased [5,9–11]. Even though an active field of research currently centers on hUC-MSCs, thus far there is no consensus on the optimal method to isolate, expand and characterize hUC-MSCs. This hampers comparability and reproducibility of results obtained from studies using hUC-MSCs.

The isolation and expansion of hUC-MSCs is a multi-step process. After birth, the UC is collected and stored under conditions that maintain cord quality for subsequent MSC isolation. After transfer to a cell culture facility, the UC is inspected and prepared for culture. The UC tissue is then cultured to allow for migration of MSCs out of the UC pieces. Upon completing subsequent MSC expansion, the cells are cryopreserved for downstream applications, including full characterization. Variable protocol choices in each phase of the procedure may impact hUC-MSC characteristics, which is why optimization and standardization at every step of the process is essential.

Many different protocols describing the isolation and expansion of hUC-MSCs are used and published. These protocols vary greatly in tissue collection and preparation methods, culturing conditions and hUC-MSC characterization [8,12]. Differences in processing of the starting material can introduce persistent and unpredictable variation in the MSCs. In current published protocols, the UC collection procedure, UC storage conditions and maximum storage duration are often poorly defined [13]. Subsequent processing of the UC differs largely per isolation protocol. Some protocols advise to remove blood vessels from the cord before MSC isolation [14–17], whereas others culture the cord including veins and arteries [10,18,19]. In addition, the MSC-isolation procedures from UC differ widely, where the culture of larger explants [18,20], smaller “fine-piece” explants [11,16,17,19,21] as well as enzymatic digestion [10,11,16,17,22] are among the most commonly used isolation techniques. During isolation and expansion, different culture media and various types and concentrations of serum and other medium supplements are used [13,23]. Also, seeding densities vary between protocols, yet harvesting confluence remains similar among protocols [19,23]. Variability at each of these steps can affect hUC-MSC characteristics, such as growth kinetics and morphology, among others, due to their effects on their molecular profile (e.g., transcriptome, methylome) [8,11,15]. In order to generate reproducible results and compare hUC-MSCs obtained from different donors and studies, it is key to maintain the underlying molecular profile while reducing variability resulting from environmental factors.

MSCs are characterized by their adherence to plastic, the expression of cell surface markers CD105, CD73, and CD90, while lacking hematopoietic markers such as CD45, and their capacity to differentiate into adipocytes, osteoblasts and chondrocytes [24,25]. For hUC-MSC isolation, protocols generally have an adherence-based selection method [26]. Although, phenotype analysis and assessment of differentiation capacity varies greatly between studies, cell surface expression of CD73, CD90, CD105 and CD45 is consistently assessed. However, in-depth immunophenotypic analyses are highly variable and appear unmethodical. Besides, the used antibody concentrations and analysis strategies are often not standardized within or between research groups, thereby impairing comparison of the generated results [12,13,23,25–27]. Similarly, regarding the differentiation capacity of hUC-MSCs, a range of contradictory results have been published. Although some studies present an excellent differentiation capacity, others describe the inability to differentiate into any of the three lineages, leaving the actual capacity for trilineage differentiation indeterminate [19,21,28–30].

To enhance the robustness and reproducibility of hUC-MSC–derived results between donors within a study cohort and between studies from different research groups, it is crucial to standardize hUC-MSC isolation and expansion protocols. By comparing, selecting and optimizing variables at each step of this procedure, we have developed and standardized a method for the isolation, expansion and characterization of hUC-MSCs. Using an extended population of 90 donors, we isolated and expanded MSCs from UCs to show reproducibility of our method.

Materials and Methods

Ethical statement

hUCs were collected at the department of obstetrics at the Leiden University Medical Center in the Netherlands with ethical approval of the institutional medical ethical committee (P18.184). Written informed consent for the collection of hUC for research purposes was obtained from all parents. Mothers were included when diagnosed with a monochorionic twin pregnancy in the framework of the Twinlife study (International Clinical Trials Registry Platform ID NL7538) [31].

UC donor characteristics

All UC samples were derived from monochorionic twin pregnancies [31]. Per pregnancy, one individual of each twin pair was included in the analysis. The first presenting fetus of which the placental cord insertion during pregnancy was closest to the maternal cervix at first ultrasound was used for analysis, as this is considered a random characteristic. In total, UCs from 90 donors were included (female, 47 [52%], delivery by cesarean section, 59 [66%]). The median gestational age at birth was 33.8 weeks (range, 25.9–37.0 weeks; interquartile range [IQR], 30.4–36.1 weeks). The median birth weight was 1853 g (range, 660–3330 g; IQR, 1376–2362 g).

UC collection and processing

At least 5 cm of the hUC was collected as soon as possible, with a maximum of 6 h after vaginal or cesarean delivery in collection buffer (phosphate-buffered saline [PBS]) supplemented with 0.38 μg/mL polymyxin B-sulphate (Sigma-Aldrich, St. Louis, MO, USA), 20 μg/mL kanamycin (Gibco/Thermo Fisher Scientific, Waltham, MA, USA), 10 μg/mL penicillin/streptomycin (Lonza, Basel, Switzerland) and 1 μg/mL Amphotericin-B (Sigma-Aldrich). The hUC was kept in collection buffer at 4°C until processing. Before processing, characteristics of the hUC were documented, including appearance, length of the collected hUC (centimeters), thickness (centimeters), coiling (intensity scale 1-5), the amount of blood clots (intensity scale 1–5) and edematous Wharton’s Jelly (intensity scale 1–5). Thereafter, the hUC was cut into 2-cm segments and washed in sterile PBS until all superficial blood clots were removed. The hUC pieces were transferred onto a Petri dish on ice and cut longitudinally to expose the umbilical arteries and vein. The blood vessels and remaining blood was removed as much as possible. Additional superficial incisions were made on the inside of the cord to increase the tissue surface and adherence. Approximately six dissected hUC pieces of ~1 cm^2 surface with a height of 3–5 mm were transferred into a sterile 10-cm Petri dish with the inside of the cord (Wharton’s Jelly) facing down. Cord pieces were left to adhere to the plastic for 20 min at room temperature

(RT) before ~8 mL of culture medium was added. The culture medium level did not exceed the height of the hUC pieces to prevent detachment of the cord from the dish. Subsequently, the dishes were incubated in a humified atmosphere at 37°C with 5% CO_2.

hUC-MSC isolation and culture

Minimum essential medium α (αMEM) GlutaMAX (Gibco) was used as standard culture medium supplemented with 100 μg/mL penicillin/streptomycin (Gibco) and 5% PLTGOLD human platelet lysate (hPL) (Merck, Rahway, NJ, USA). Where stated otherwise, Dulbecco's Modified Eagle's Medium (DMEM) GlutaMAX (Gibco) supplemented with 100 μg/mL penicillin/streptomycin and 10% fetal bovine serum (FBS) (Sigma) was used. Culture medium was changed twice a week.

Outgrowth of the hUC-MSCs is mainly visible at the perimeter of the explants. When more than one-half of the forming hUC-MSC patches showed a confluence of >70%, the explants were removed, and the dish was washed twice with PBS. hUC-MSCs were dissociated using TrypLE Select (Gibco). Total cell count and viability were established using a hemocytometer. Subsequently, the cells were seeded into a culture flask at a density of 2500/cm^2. When the hUC-MSC reached a confluence of >70%, the hUC-MSCs were dissociated from the plate using TrypLE Select. Passage 1 cells were used for experiments unless stated otherwise. The absence of mycoplasma was confirmed by polymerase chain reaction (PCR).

Phenotype assessment by flow cytometry

hUC-MSCs were stained with saturating quantities of CD73 (AD2, BV421), CD90 (5E10, PerCP-Cy^{TM}5.5), CD105 (SN6, FITC), CD45 (2D1, APC-H7) and CD31 (WM59, APC) monoclonal antibodies and the LIVE/DEAD stain kit (Invitrogen, Carlsbad, CA, USA) according to the manufacturer's protocol. Cells were analyzed using the FACSCanto I Flow Cytometer using FACSDiva software for acquisition. Flow cytometer settings were performed as previously described [32]. Data were analyzed using BD FlowJo, version 10, software, as shown in Supplementary Figure 1.

Adipogenic differentiation and Oil-Red-O staining

For adipogenic induction, 2500 cells/cm^2 (bone marrow [BM]-MSCs) or 640 cells/cm^2 (hUC-MSCs) were cultured in adipogenic induction medium containing DMEM GlutaMAX supplemented with 100 μg/mL penicillin/streptomycin, 10% FBS, 10 μmol/L dexamethasone (Sigma-Aldrich), 10 μg/mL insulin (Sigma-Aldrich), 5 μmol/L 3-sobutyl-1-methylxanthine (Sigma-Aldrich), 50 μmol/L indomethacin (Sigma-Aldrich) and 1 μmol/L rosiglitazone (Sigma-Aldrich). The medium was refreshed twice a week. After 21 days of differentiation, lipids and neutral triglycerides were stained using Oil-Red-O. For this purpose, the cell monolayer was washed twice with PBS, before a 15-min fixation with 4% formaldehyde. Fixation is followed by two washes with PBS, one with milliQ and a short wash with 60% isopropanol. Afterwards, the lipids were stained for 10 min with a filtered Oil-Red-O working solution consisting of three volumes 0.5% Oil-Red-O (Sigma-Aldrich) in isopropanol and 2 volumes milliQ. Excess staining was removed by a short wash with 60% isopropanol and three washes with milliQ, before the cells were imaged with the Olympus CKX53. Control bone marrow-derived MSCs were isolated as previously described [33].

Osteogenic differentiation, alkaline phosphatase (ALP) and Alizarin Red S staining

For osteogenic induction, 2500 cells/cm^2 (BM-MSCs) or 640 cells/cm^2 (hUC-MSCs) were cultured in osteogenic induction medium containing αMEM GlutaMAX supplemented with 100 μg/mL penicillin/streptomycin, 5% PLTGold hPL, 10 μmol/L dexamethasone, 5 μg/mL L-ascorbic acid (Sigma-Aldrich) and 5 mmol/L β-glycerophosphate (Sigma-Aldrich). The medium was refreshed twice a week. After 21 days of differentiation, the ALP activity and calcium deposition were visualized. Before staining, the cells were washed twice with PBS and once with milliQ. For the ALP staining, first a solution of 40 mg/mL Naphthol AS-MX phosphate disodium salt (Sigma-Aldrich) in N,N dimethylformamide (Sigma-Aldrich) was prepared, which is used to dissolve 120 mg/mL Fast blue RR salt (Sigma-Aldrich). For each milliliter of this solution, 100 mL of 0.2 mol/L Tris, pH 8.9 (Thermo Fisher Scientific), was added, followed by 100 mL of milliQ and 2 mL of $MgSO_4$ (Sigma-Aldrich). Thereafter, the solution was filtered through a 0.2-μm filter. To then visualize the ALP activity, the cells were incubated for 5 min at RT in the ALP staining solution and washed twice with PBS before imaging with the Olympus CKX53. To visualize the calcium deposition, the cells were fixed with 70% ethanol for 1 h at −20°C and then rehydrated with milliQ for 3 min at RT. After, the cells were incubated with Alizarin Red S solution (Sigma-Aldrich) for 10 min at RT. For removal of the excess staining, the cells were washed three times with milliQ before imaging with the Olympus CKX53.

Chondrogenic differentiation and Alcian Blue staining

Chondrogenesis was induced in 3D pellets as previously described [34]. For this purpose, 2.5 × 10^5 MSCs were pelleted in 15 mL of polypropylene conical tubes (260 xg, 5 min). After overnight incubation, the standard culture medium was replaced with a serum-free chondrogenic induction medium consisting of DMEM GlutaMAX, 100 μg/mL penicillin/streptomycin, 50 μg/mL L-ascorbic acid, 0.1 μmol/L dexamethasone, 40 μg/mL L-proline (Sigma-Aldrich), 100 μg/mL sodium pyruvate (Sigma-Aldrich), 10 μL/mL ITS-Plus (Sigma-Aldrich) and 10 ng/mL hTGF-β1 (Tebu-bio, Ile de France, France) [34]. The chondrogenic culture medium was refreshed twice a week for a period of 5 weeks, of which from the second week onwards hypoxic conditions were applied. Thereafter, the diameter and surface area of the pellets was assessed microscopically using the Olympus BX53. The pellets were then fixed in 4% formaldehyde at 4°C overnight. Subsequently, the pellets were washed with 50% ethanol and stored in 70% ethanol until dehydration with an automated tissue processer and paraffin embedding. Sections of 5 μm were mounted on a glass slide and deparaffinized by incubating the slides twice in Histo-Clear (10 min; National Diagnostics, Atlanta, GA, USA), twice in 100% ethanol (5 min), once in 96% ethanol (3 min), once in 70% ethanol (3 min), once in 50% ethanol (3 min) and once in milliQ (3 min). To visualize the deposited glycosaminoglycans, the slides were primed for 5 min in 0.1 N HCl (J.T. Baker, pH 1, 5 min), followed by a 30-min incubation in a 1% Alcian Blue 8-GX solution in 0.1 N HCl (Sigma-Aldrich). Excess staining was removed by 10 min of incubation with 0.1 N HCl and rinsing followed by a 30-min incubation with milliQ. Counterstaining was performed with a subsequent incubation in Nuclear Fast Red (Sigma-Aldrich). After 5 min, the slides were rinsed with milliQ (5 min) and dehydrated with 50% ethanol, 70% ethanol, 100% ethanol and Histo-Clear (1.5 min each), before the slides were mounted with Pertex (HistoLab, Brea, CA, USA) and imaged with the Olympus BX35.

RNA isolation, reverse transcription and real-time quantitative PCR

Cells derived from monolayer cultures were harvested, washed and snap frozen as a pellet in liquid nitrogen. RNA was isolated using the Zymo *Quick*-RNA Microprep Kit (Zymo Research, Irvine, CA, USA) according to the manufacturer's protocol. RNA concentration was assessed using Qubit RNA BR Assay Kits (Life Technologies, Carlsbad, CA, USA). To synthesize cDNA, the Transcription First Strand cDNA synthesis kit (Roche, Basel, Switzerland) was applied according to the

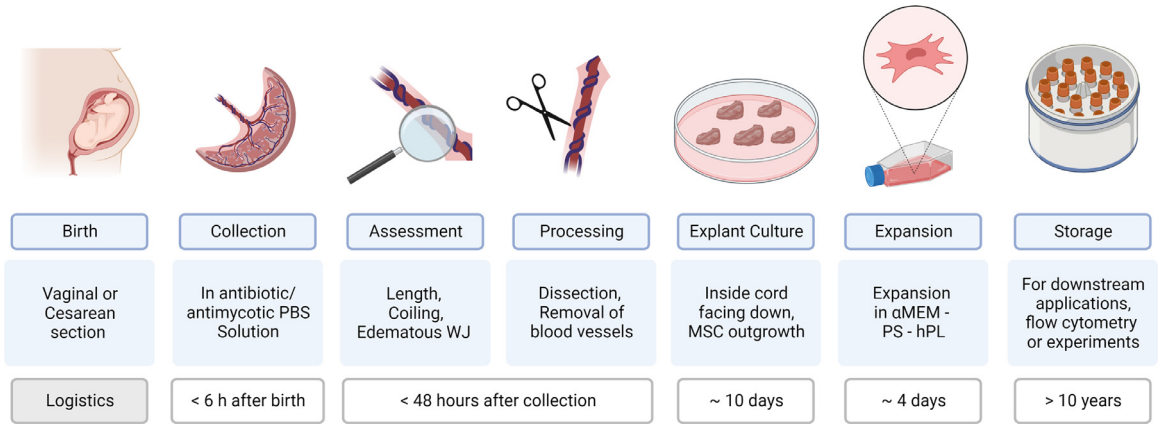

Figure 1. Schematic overview of the standardized protocol to isolate MSCs from the UC. All stages of the MSC-isolation process including the collection and assessment of the UC, the generation of explant from the UC, and the expansion and storage the isolated hUC-MSCs are depicted. The time required for each individual step of the process is indicated in the bottom row. PS, penicillin–streptomycin; WJ, Wharton's jelly.

provided protocol using 200 ng of RNA as input. Each 10-μL PCR contained 2.5μL Taqman Fast Advanced Master Mix (Applied Biosystems, Waltham, MA, USA), 0.5 μL of Taqman Gene Expression assay, 0.5 μL of cDNA and 6.5 μL of milliQ. Taqman Gene Expression Assay IDs were Hs01047975_m1 (*RUNX2*), Hs00939627_m1 (*GUSB*, Housekeeping gene), Hs01122454_m1 (*YWHAZ*, Housekeeping gene). The PCR was run on the QuantStudio 6 Flex (Applied Biosystems) for 2 min at 50°C, for 20 s at 95°C, followed by 40 cycles of 1 s at 95°C and 20 s at 60°C. Each condition was run in triplicate. The average of the technical replicates was only used for analysis when the standard deviation of the technical replicates did not exceed 0.5. The fold change was calculated by the $2^{-\Delta\Delta Ct}$ method.

Inhibition of T-cell proliferation

Peripheral blood mononuclear cells (PBMCs) were isolated from buffy coat of anonymous blood bank donors (Sanquin, Amsterdam, The Netherlands), using Leucosep centrifuge tubes according to the manufacturer's protocol (Greiner Bio-One, Kremsmünster, Austria). Subsequently, the PBMCs were stimulated with Human T-Activator CD3/CD28 Dynabeads (Thermo Fisher Scientific) (5 μL/10^6 PBMCs) and cultured in the presence of passage 2 hUC-MSCs for 5 days at 37°C and 5% CO_2. PBMC to hUC-MSC co-culture ratios of 1:2, 1:8, 1:32, 1:128 and 1:512 were assessed. Unstimulated PBMCs served as a negative control, whereas CD3/CD28 stimulated PBMCs served as a positive control. Thereafter, the cultures were incubated overnight with 3H-thymidine. Incorporation of the 3H-thymidine was measured and displayed as a percentage of the positive control.

Data analysis and visualization

The associations between MSC characteristics and the attributes of donors and hUCs were quantified using the Spearman's rank correlation. The *P*-values were Bonferroni corrected and considered statistically significant when < 0.05. Differences in population doubling time, population doubling level, surface marker expression, cumulative cell count and viability between culture conditions (with/without blood vessels; αMEM-hPL/DMEM-FBS) were tested using a two-sided paired *t*-test. Differences in surface marker expression and T-cell proliferation inhibition capacity between short- and long-term cryopreserved hUC-MSCs were tested using a two-sided unpaired *t*-test. Statistical analyses were performed using R software, version 4.1.0. Graphs and figures were created using R Software, version 4.1.0, and BioRender (https://biorender.com/).

Results

Standardized isolation and expansion of MSC from 90 UCs

To develop a method for the standardized isolation and expansion of hUC-MSCs, we used a series of cords obtained from 90 donors. The isolation and expansion of MSCs from UC is a multi-step process spanning multiple days. Herein, we summarize the isolation and expansion method after protocol optimization (Figure 1).

UCs obtained from 90 donors after cesarean or vaginal delivery were collected within 6 h (median 0.6 hours) after birth and stored in an antibiotic/antimycotic solution (collection buffer). The MSC isolation process was initiated within 48 h (median, 17 h) after collection (Table 1). A morphological assessment of the UC was performed. Thereafter, the blood vessels and residual blood were removed and UC pieces of ~1 cm^2 (UC explants) were plated onto a culture dish.

After approximately 3 days of culture in the presence of human platelet lysate supplemented culture medium, it was observed that the first MSCs migrated out of the UC explants. In the subsequent week, the number of hUC-MSCs surrounding the cultured explants increased and confluent colonies were formed. Blood cells were observed throughout the first week of culture and diminished upon subsequent culture medium changes (Figure 2).

After a median culture period of 10 days (IQR, 9.0–11.0 days, Table 1), more than 50% of the MSC colonies reached a confluence of >70%. At this stage, UC pieces were removed and passage 0 (P0) hUC-MSCs were transferred to a culture flask and expanded for an additional passage. The number of cells obtained per UC explant (median 21.5 $\times$ 10^3 cells) varies greatly between the individual donors despite the highly comparable initial amount of tissue used for culture initiation (IQR, 14.3–39.7 $\times$ 10^3 cells, Table 1). The viability of the P0 hUC-MSCs was comparable between the donors (median, 97.2%; IQR, 95.9–98.4%, Table 1).

The passage 1 (P1) cultures were assessed daily for confluence. When reaching a confluence of >70% (median, 4 days; IQR, 4–4 days), hUC-MSCs were harvested. The population doubling level (PDL; median, 4.8 doublings; IQR, 4.5–5.1 doublings) and population doubling time (PDT; median, 0.9 days; IQR, 0.8–0.9 days) were comparable across the 90 hUC-MSC isolates (Table 1). A median of 99% of the cells (IQR, 98.6–99.2) expressed the cell surface markers CD73, CD90 and CD105 and did not express CD45 and CD31 (Table 1). The cell surface marker expression did not differ ($P = 0.59$) between short- (mean, 0.6 months) and long-term (mean, 21 months) cryopreserved samples (Supplementary Figure 2A). Combined, this indicates that this method allows for the reproducible isolation and expansion of hUC-MSC across UC donors.

Table 1
Umbilical cord collection and MSC characteristics.

Characteristic	Median (n = 90)	Interquartile range	Minimum–maximum
Umbilical cord collection			
Time between birth and umbilical cord collection, h	0.6	0.5–0.75	0.0–6.0
Time between collection and umbilical cord processing, h	17.1	10.5–24.8	1.0–47.5
Mesenchymal stromal cells			
Days in passage 0	10.0	9.0–11.0	6.0–16
Cells obtained per UC piece Passage 0 ($\times 10^3$)	21.5	14.3–39.7	01.5–154
Cumulative cell count per UC piece Passage 1 ($\times 10^2$)	67.5	36.8–121.7	3.8–730.8
Viability passage 0	97.2	95.9–98.4	86.0–100
Viability passage 1	97.9	96.5–98.7	84.5–100
Fold expansion passage 1	28.7	23.3–33.8	10.9–84.6
PDT passage 1	00.9	0.8–0.9	0.6–1.5
PDL passage 1	04.8	4.5–5.1	3.4–6.4
$CD73^+$ passage 1, %	99.8	99.8–99.9	99.1–100
$CD90^+$ passage 1, %	99.9	99.8–99.9	99.1–100
$CD105^+$ passage 1, %	99.3	99.0–99.4	97.2–99.8
$CD45^+$ passage 1, %	00.16	0.11–0.28	0.04–2.3
$CD31^+$ passage 1, %	00.07	0.05–00.1	0.01–1.73
$CD73^+$, $CD90^+$, $CD105^+$, $CD45^-$, $CD31^-$ passage 1, %	98.9	98.6–99.2	96.8–99.6

Characteristics of the umbilical cord collection and of the mesenchymal stromal cells are shown.
MSC, mesenchymal stromal cell; PDL, population doubling level; PDT, population doubling time.

hUC-MSCs culture characteristics show limited donor-to-donor variability

Donor characteristics such as birth weight, gestational age, sex and mode of delivery could affect hUC-MSC culture characteristics and may thereby impede comparability of cells obtained from different donors. To assess the potential impact of donor characteristics on the hUC-MSCs cultured using our method, birth weight, gestational age, sex and mode of delivery were correlated with outgrowth parameters and hUC-MSC properties. No associations were found between the donor characteristics and the number of hUC-MSCs obtained per UC explant or the hUC-MSC viability, indicating the robustness of our protocol. Notably, a lower gestational age ($P = 2.6 \times 10^{-4}$), a lower birth weight ($P = 2.1 \times 10^{-3}$) and delivery by cesarean section ($P = 8.7 \times 10^{-5}$) significantly correlated with decreased number of days needed to conclude hUC-MSC outgrowth in P0 (Figure 3).

Time limits for UC collection and storage

Cord handling before MSC isolation is a two-step process. After birth, the UC is cut to discontinue the blood flow between placenta and newborn. Thereafter, the UC is cut from the placenta and placed in the collection buffer to decelerate dehydration and cell death. Second, the UC is stored at 4°C until processing. Since an increased collection and storage time may affect hUC-MSC characteristics such as viability, it is critical to establish time limits for these steps. We assessed whether a collection and storage time of up to 6 and 48 h, respectively, is associated with changes in hUC-MSC outgrowth efficiency and characteristics. Neither the time required for hUC-MSC outgrowth, retrieved number of cells per explant, viability nor the PDT, PDL or immunophenotype correlated with the passed time between birth, collection and processing (Figure 3). This indicates that it is feasible to collect the UC up to 6 h after birth and store the UC for up to 48 h after collection without altering hUC-MSC characteristics and outgrowth performance. It should be noted however, that 89% (80) of the UCs were collected within one hour after birth whereas merely 3% (3) of the UCs were collected 4 or more hours after birth, resulting in a lower sensitivity to test the effect of moderate delays in collection on hUC-MSCs culture.

Variation in UC characteristics do not associate with hUC-MSC properties

Every umbilical cord has a unique morphology (Figure 4). The extent of coiling, edematous Wharton's jelly and blood vessel visibility vary greatly among UCs (Figure 4), and this may affect the full removal of the arteries and vein during UC dissection. Also, we observed that the presence of blood clots and high mucinousity is a predictive factor for blood cell contamination in the first week of culture. Differences in UC morphology and explant composition may introduce heterogeneity in culture conditions and as such affect hUC-MSC characteristics and purity. To assess the potential impact of UC composition on the hUC-MSCs obtained using our method, all UC characteristics were mapped before processing, including the extent of coiling, blood clots, mucinousity, edematous Wharton's jelly and visibility of blood vessels. Next, these were correlated with the hUC-MSC characteristics, growth performance and population purity. No significant associations were identified. Neither the time required for hUC-MSC outgrowth, retrieved number of cells per explant, hUC-MSC viability nor the PDT, PDL or the expression of cell surface markers were affected by variations in UC morphology (Figure 3). Taken together, with our method hUC-MSC characteristics are stable and yield robust results across all hUC-types.

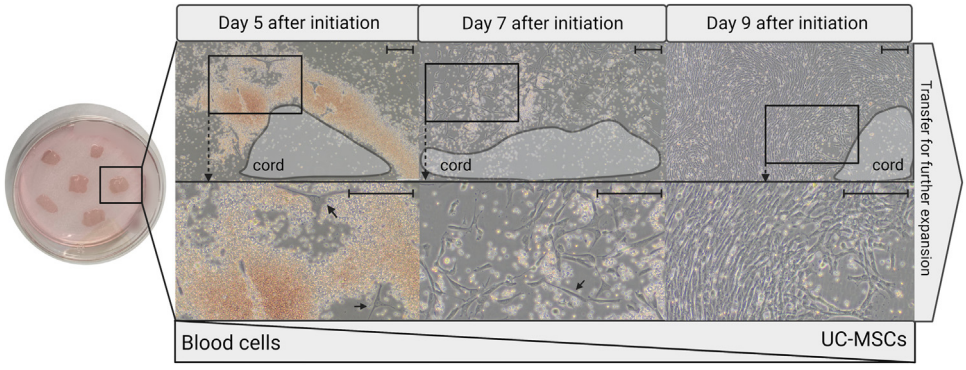

Figure 2. MSC outgrowth from the UC. Visualization of the outgrowth of MSCs from the UC. Explants are plated on a dish (10 cm) with the inside of the cord facing down. After approximately 3 days, individual MSCs become visible at the explant perimeter Over time, the blood cell presence decreases and the MSCs expand, forming colonies along the explant perimeter. Before imaging, the cord was removed from the dish for optimal contrast. The location of the cord explant is indicated by gray lining. Solid arrows indicate MSCs. The boxes and dashed arrows indicate the location of which the enlarged image is depicted below. Scale bars indicate 200 μm.

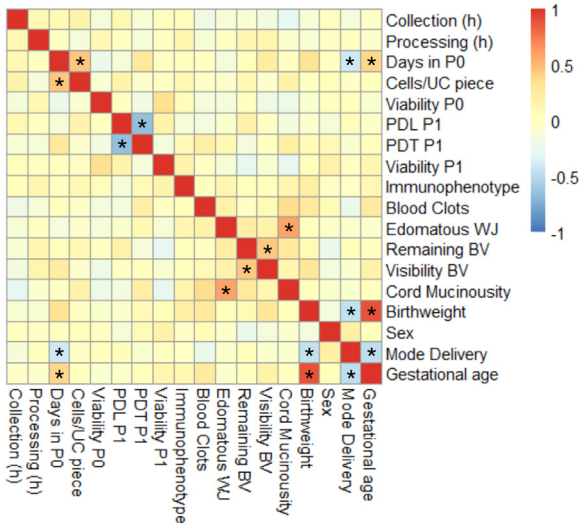

Figure 3. Donor characteristics, UC phenotype and processing variables are not associated with the characteristics and performance of hUC-MSCs. Shown is a correlation heatmap of variables associated with the UC donor, UC processing, the UC phenotype and UC-derived MSCs. Legend indicates strength of correlation (red: high positive correlation; yellow: weak correlation; blue: strong negative correlation). N = 90. Spearman's rank correlation was used. *P*-values were considered significant (indicated by asterisk*) when < 0.05 after Bonferroni correction. "Immunophenotype" indicates the percentage cells positive for CD73, CD90 and CD105 while negative for CD45 and CD31. BV, blood vessels; P0, Passage 0; P1, Passage 1; WJ, Wharton's jelly.

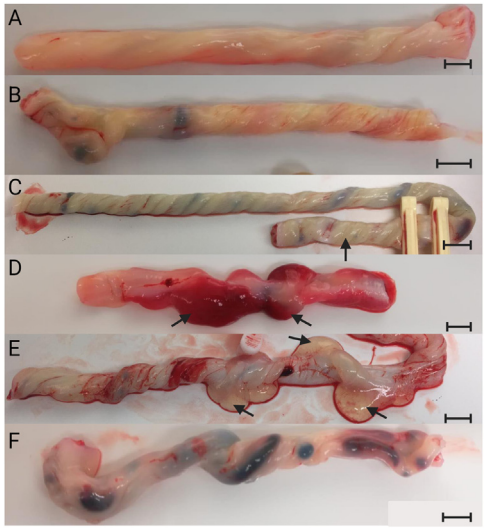

Figure 4. Differences in UC morphology. (A) Normal coiled hUC with no visible blood clots or edematous Wharton's jelly and a very low degree of mucinousity. (B) Normal coiled hUC with few blood clots, no edematous Wharton's jelly, a false knot (left) and a low degree of mucinousity. (C) Hypercoiled hUC with clearly visible blood clots and a low degree of mucinousity. (D) Normal coiled hUC with high amount of blood containing Wharton's jelly, and a very high degree of mucinousity. (E) Normal coiled hUC with a high amount of edematous Wharton's jelly, medium degree of mucinousity. (F) Normal coiled hUC with a high amount of clearly visible blood clots, no edematous Wharton's jelly, a false knot and a low degree of mucinousity. Black arrows indicate edematous Wharton's jelly. Scale bar indicates 1 cm.

Blood vessel removal before culture improves purity of hUC-MSC isolates

The presence of blood and endothelial cells in hUC-MSC cultures may alter cell-type composition and hUC-MSC characteristics. However, a complete blood vessel removal from the explants cannot always be guaranteed as UC morphology can complicate blood vessel dissection. To assess the effect of blood vessel presence on hUC-MSC isolation, expansion, and purity, explants obtained from three random donors were each cultured with and without blood vessels. Subsequently, hUC-MSC characteristics and purity were compared between the three selected donors of each group. At P0, more blood cells were observed in the dishes with explants of which the blood vessels were not removed (Figure 5A). Also, an increased percentage of $CD45^+$ leukocytes and $CD31^+$ endothelial cells was observed in these cultures (Figure 5B). However, this percentage was highly variable between the three donors (90.6%-97.9%). Leukocytes and endothelial cells disappeared after P0 and were not detected in the P1 hUC-MSC populations (Figure 5B, Supplementary Figure 3C). hUC-MSCs derived from hUC explants with and without blood vessels exhibited the typical elongated, fibroblastic-like spindle-shaped morphology. The hUC-MSCs did not differ in size, granularity or complexity between the two conditions (Figure 5A, Supplementary Figure 3). Also, the PDL and PDT were comparable, and the cultures derived from both dissection methods yielded comparable numbers of cells with a similar viability for at least three passages.

Thus, retaining the blood vessels in the explant during isolation did not impact proliferation capacity, cell counts and viability but led to a greater frequency of leukocytes and endothelial cells at P0. Therefore, we included the dissection of blood vessels from the UC-tissue before culture initiation in our method to avoid leukocyte and endothelial cell contamination. Small blood vessel fragments that might remain in the explants after dissection did not appear to affect hUC-MSC characteristics and can therefore be disregarded.

Culture in αMEM-hPL yields hUC-MSCs with a consistent growth performance and characteristics compared with DMEM-FBS

Culture medium and supplement may impact on MSC growth performance and characteristics [10,35,36]. To determine which culture medium and supplement yields the most consistent hUC-MSC growth performance and characteristics, we compared the two most commonly used medium-supplement combinations: αMEM supplemented with hPL (αMEM-hPL) and DMEM supplemented with FBS (DMEM-FBS) [37]. hUC-MSCs obtained from three different random donors were isolated, expanded in each medium for a duration of 6 passages and compared. hUC-MSCs exhibited distinctive differences when isolated and expanded in αMEM-hPL or DMEM-FBS culture medium. hUC-MSCs of the three selected donors isolated and cultured in αMEM-hPL continuously displayed typical elongated spindle-shaped fibroblastic-like MSC morphology. Although, hUC-MSCs became increasingly irregular and variable in size and shape in prolonged cultures, exhibiting a more flattened morphology with increased protrusions. hUC-MSCs of the three donors derived from DMEM-FBS cultures also showed a typical fibroblastic-like MSC morphology, but as compared with the αMEM-hPL-hUC-MSCs, show an increased granularity, size, and filamentous appearing cytoplasm. The increase in irregular shape and size over time was more evident and appeared at an earlier passage as compared with αMEM-hPL-hUC-MSCs (Figure 6A).

The time required for P0, and population doubling was increased in hUC-MSCs cultured in DMEM-FBS as compared with those isolated and expanded in αMEM-hPL, whereas the number of cells retrieved per explant as well as the PDL were decreased (Figure 6C,D). Consequently, explants cultured in DMEM-FBS yielded considerably less hUC-MSCs (Figure 6B). Moreover, slightly lower viability was observed in DMEM-FBS-hUC-MSCs until passage 3, at which time point the viability of the αMEM-hPL-hUC-MSCs also started to decline (Figure 6E).

An increased percentage of $CD45^+$ leukocytes and $CD31^+$ endothelial cells was observed in P0 of DMEM-FBS-hUC-MSCs as compared with P0 αMEM-hPL-hUC-MSCs (Figure 6F, Supplementary Figure 4). In conclusion, the isolation and expansion in αMEM-hPL resulted in hUC-MSCs with a homogenous morphology and yielded a greater number of cells, increased viability and lowered PDT as compared with DMEM-FBS. Therefore, αMEM supplemented with hPL was selected as culture medium in our method.

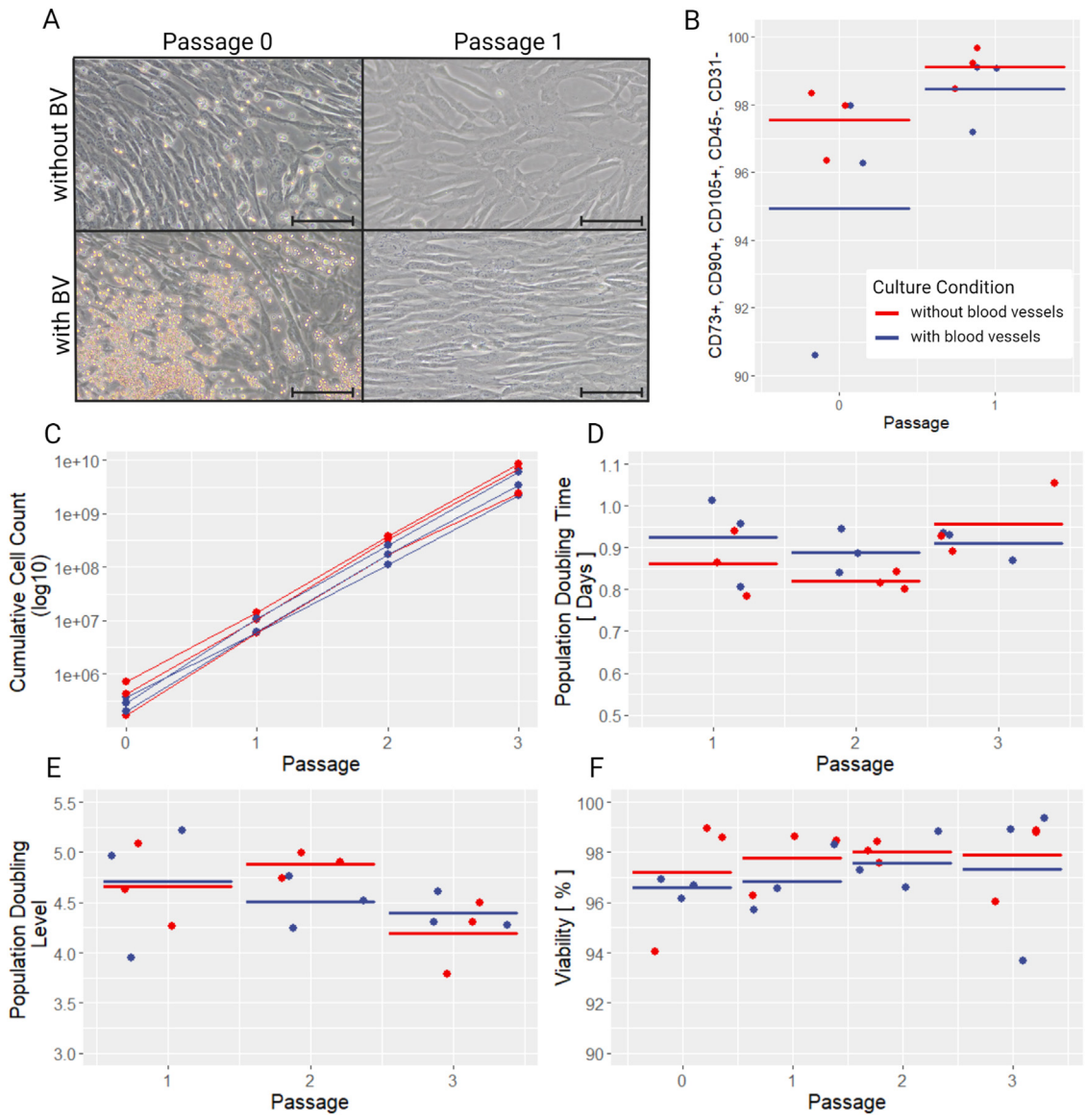

Figure 5. Comparison of MSCs derived from explants with and without blood vessels. (A) Morphology of MSCs derived from explants with and without blood vessels. Scale bars indicate the 200 μm. (B) Percentage of CD73+, CD90+, CD105+, CD45− and CD31− cells. (C) Cumulative cell count of the MSCs derived from 18 umbilical cord explants (~1 cm^2) until passage 3. (D) Population doubling time, (E) population doubling level and (F) viability of hUC-MSCs derived from explants with (blue) and without (red) blood vessels. Crossbar displays the mean of the individual values of the three donors (dots). No statistically significant differences were observed between the culture conditions (paired two-sided *t*-test).

Trilineage differentiation capacity of hUC-MSCs as compared with BM-MSCs

MSCs are generally characterized by the capacity to differentiate into adipocytes, osteoblasts, and chondrocytes (Figure 7A) [25]. Therefore, we assessed the differentiation capacity of hUC-MSCs obtained from three random donors. BM-MSCs were used as positive control and undifferentiated MSCs were used as negative controls.

Over the course of the 3 weeks of adipogenic differentiation, the morphology of hUC-MSCs changed from a typical fibroblastic-like morphology towards highly irregular shaped cells with notably granular cytoplasm. Also, a greater content of neutral triglycerides and lipids as compared with the undifferentiated control was detected with Oil-Red-O staining. However, the typical fat storage in vesicles was absent in differentiated UC-MSCs, whereas this was observed in the differentiated BM-MSCs (Figure 7B).

After 3 weeks of osteogenic differentiation, hUC-MSCs showed no calcium deposition and little ALP activity. In contrast, differentiated BM-MSCs show a considerable amount of calcium deposition and ALP activity (Figure 7B). The hUC-MSCs kept expanding throughout the differentiation process and did not show signs of growth inhibition, as normally seen in these kinds of cultures. Gene expression analysis of the early osteogenic transcription factor *RUNX2* was, however, increased in all differentiated hUC-MSC lines as compared with the control, compatible with early activation of the differentiation pathway. The differentiated BM-MSCs did not show elevated gene expression for *RUNX2,* possibly because their differentiation stage had passed the phase of *RUNX2* upregulation (Figure 7C).

Prolonged three-dimensional chondrogenic differentiation over a 5-week period resulted in hUC-MSCs featuring an increased deposition of matrix as compared with the undifferentiated control cells. This was visualized by the staining of the main matrix components of cartilage tissue, glycosaminoglycans (Figure 7B). Also, the size of the three-dimensional pellet was consistently increased for all differentiated pellets as compared with the control pellets, indicating an increased deposition of extracellular matrix. The amount of matrix deposition reached after differentiation of BM-MSCs however was considerably more prominent as compared with UC-MSCs

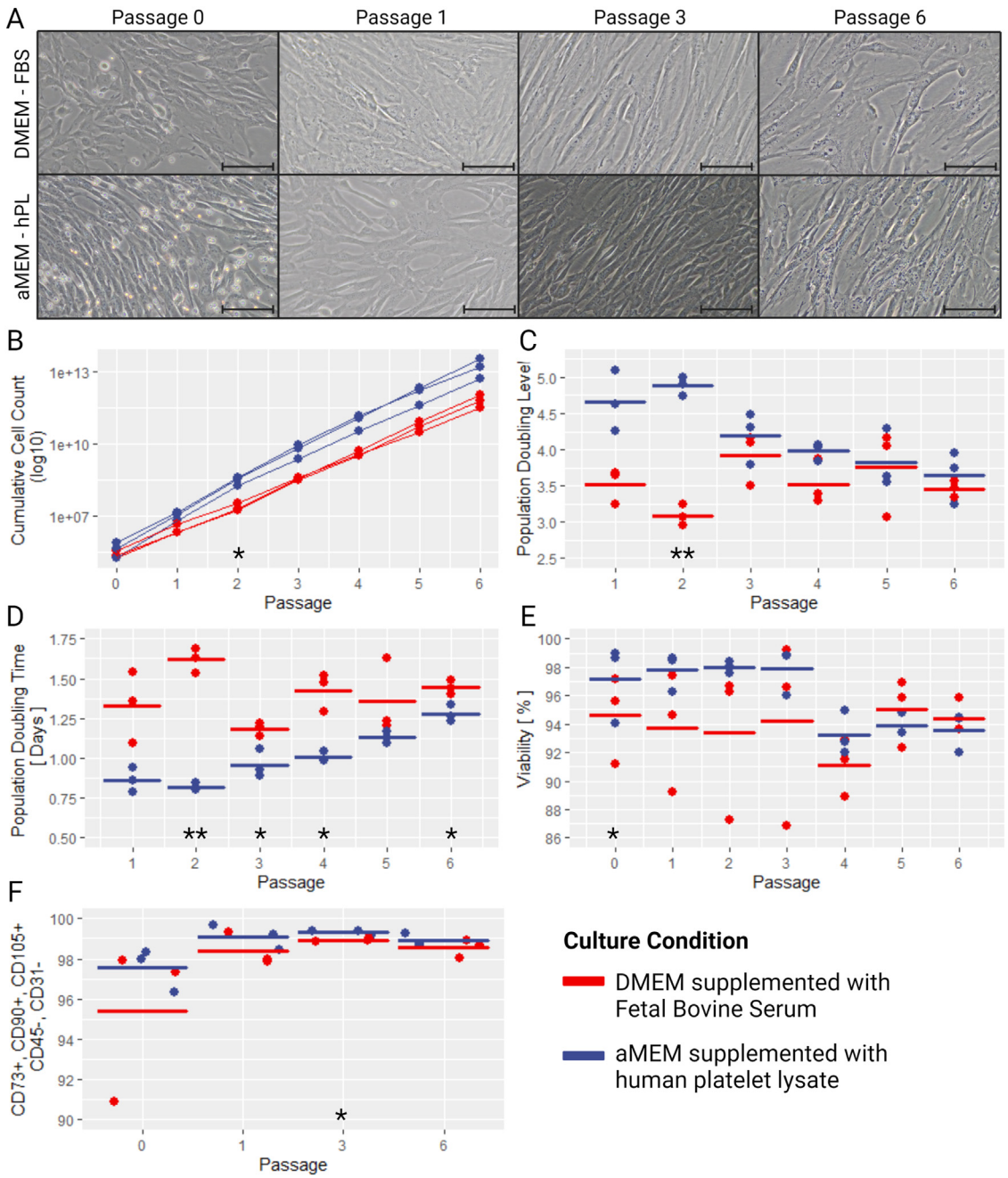

Figure 6. The effect of serum and culture medium choice on MSC characteristics and performance: Analysis of hUC-MSCs isolated and expanded in either DMEM supplemented with FBS (indicated in red) or αMEM supplemented with hPL (indicated in blue) until passage 6. (A) Morphology. Scale bars indicate 200 μm. (B) Cumulative cell count of the MSCs derived from 18 umbilical cord pieces (~1 cm^2) until passage. (C) Population doubling level. (D) Population doubling time. (E) Viability. (F) Percentage of CD73+, CD90+, CD105+, CD45-, CD31- cells. Crossbar displays the mean of the individual values of the three donors (dots). A paired two-sided *t*-test was used to test for statistically significant differences between culture conditions: $^{*}P \leq 0.05$, $^{**}P \leq 0.01$.

(Figure 7D). Thus, UC-MSCs appear to initiate differentiation when exposed to differentiation factors, although did not effectively complete differentiation as compared with BM-MSCs in the given time using the currently available protocols for MSC differentiation.

Isolated hUC-MSCs suppress T-cell proliferation

To assess the capacity of the hUC-MSCs to inhibit T-cell proliferation, hUC-MSCs obtained from 10 donors were co-cultured with CD3/CD28-stimulated T-cells. Co-culture with hUC-MSCs suppressed T-cell proliferation in a dose-dependent manner. With a hUC-MSC: PBMC co-culture ratio of 1:2, 13% of the proliferative capacity was retained relative to the control (Figure 7E). The capacity to inhibit T-cell proliferation did not differ between long-term (mean, 34 month) cryopreserved hUC-MSCs and short-term (mean, 12 month) cryopreserved hUC-MSCs (Supplementary Figure 2C), demonstrating that the immune-modulatory capacity of the hUC-MSCs isolated and expanded using our standardized method is independent of cryostorage duration.

Discussion

We developed a robust and standardized method for the isolation and expansion of hUC-MSCs to enable the comparison of hUC-MSC characteristics of different donors between future studies. To this end, we have optimized and standardized each step in the process of

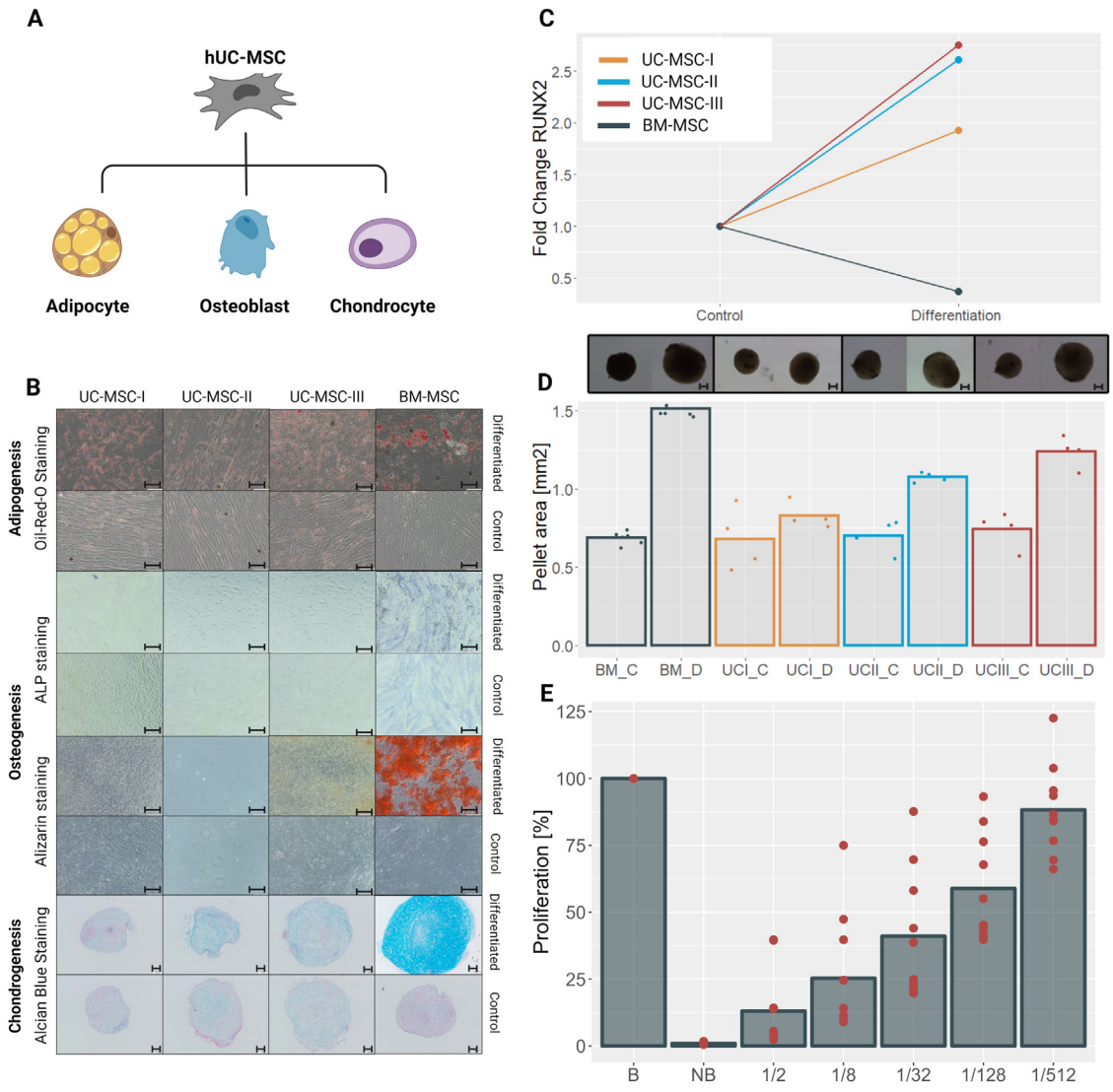

Figure 7. Functional characterization of the isolated hUC-MSCs. (A) hUC-MSCs (n = 3) and BM-MSCs (n = 1) were differentiated towards adipocytes, osteoblasts or chondrocytes. (B) Oil-Red-O staining (adipogenic differentiation, scale bars indicate 50 μm), ALP staining (osteogenic differentiation, scale bars indicate 200μm), Alizarin Red S (osteogenic differentiation, scale bar indicates 200 μm) and Alcian Blue staining (chondrogenic differentiation, scale bars indicate 100 μm) after differentiation. (C) Gene expression of transcription factor *RUNX2* after osteogenic differentiation relative to undifferentiated control. (D) Pellet area after chondrogenic differentiation. Upper row shows the microscopic image of one representative pellet per condition. Scale bars indicate 200 μm. Graph below depicts the average as well as individual values of each measured pellet. C, control; D, differentiation. (E) Inhibition of T-cell proliferation by hUC-MSCs. Bar graph displays mean of 10 donors as well as the individual measured values per donor. B, anti-CD3/CD28–stimulated PBMCs; NB, unstimulated PBMCs. Ratios indicate MSC:PBMC ratio.

MSC isolation and expansion from UC. In addition, by investigating the impact of donor heterogeneity on hUC-MSC characteristics, we were able to confirm robustness of our developed method across all donors.

We first specified time limits for the collection and subsequent storage duration of the UC before processing. After birth, a collection time of up to 6 h with an additional storage time of up to 48 h does not affect hUC-MSC isolation efficiency or characteristics, including proliferation capacity, viability and phenotype. In previously published protocols, the duration between birth and UC collection is rarely recorded [12,38]. The storage duration is more frequently described [13] and varies between 2 h [39] and 48 h [40]. Applying the presented time limits ensures that collection and storage duration does not impact on proliferation capacity, viability, and phenotype of the hUC-MSCs.

Next, we optimized the processing and isolation procedure of MSCs from UCs. Based on previously published results, we preselected the “plate-and-wait” technique to isolate UC-MSCs. With this method, explants are cultured without previous cellular dissociation by enzymatic treatment. We chose this method since enzymatic digestion has been reported to induce proteolytic stress, can result in cellular damage, and decreases cell viability [13,15–18,41,42]. Additional limitations of enzymatic digestion include degradation of cell surface receptors, alteration of cellular function, and increased PDT indicative of cellular ageing [14,16,18]. Taken together, these data favored our selection for the “plate-and-wait” technique.

In addition to the isolation procedure, the UC-processing procedures vary greatly between protocols. Although some methods include the removal of blood vessels before explant culture, others dismiss blood vessel removal as further tissue manipulation is more labor-intensive and holds a greater risk of culture contamination [13,18,43]. We found an increased number of endothelial cells and leukocytes in the hUC-MSC isolates at P0 upon retaining blood vessels in the UC explants. In line with this observation, another study employing a protocol without blood vessel removal, described residual contamination of endothelial cells in 30% of the samples at P1 [18]. In our hands, blood vessel removal before MSC isolation resulted

in a reduction of contaminating cells, including endothelial cells and leukocytes, without adverse effects on hUC-MSC characteristics and is therefore included in our method.

Another aspect we addressed is the influence of medium and medium supplements, as these are fundamental factors of variability in MSC isolation and expansion and can affect various MSC characteristics. Different media and media supplements have been used to culture MSCs [11,29,43,44]. Thus far, FBS is predominantly used as basal medium supplement. However, more recent studies are increasingly using hPL [37]. We selected αMEM-hPL as culture medium because we observed that culture in αMEM-hPL yields hUC-MSCs with a consistent growth performance and consistent characteristics as compared with DMEM-FBS. Likewise, previous studies also described favorable cell characteristics including increased proliferative capacity, decreased PDT and higher viability when comparing hPL with FBS in cultures of hUC-MSCs, BM-MSCs and adipose-tissue derived MSCs [10,35,36]. Furthermore, FBS shows a high batch-to-batch variability, requiring extensive and time-consuming comparability testing when a new batch is selected [45]. In contrast, hPL allows for increased batch-to-batch consistency and eliminates the risk of introducing animal-originating pathogens [46,47]. Also, in the view of potential clinical application of our expansion method, the use of animal components should be excluded where possible. Taken together, hUC-MSC culture in αMEM-hPL increases reproducibility and thereby comparability of results.

In addition, we standardized cell density and confluence at harvest as these can affect functional characteristics of MSCs. Seeding densities of <500 cells/cm^2 result in contact deficiency, whereas cells plated at a high density (>5000 cells/cm^2) are contact inhibited after a short culture period and must be passaged more frequently. Seeding densities of hUC-MSCs vary greatly in currently published protocols, describing densities from 100 cells/cm^2 to up to 1×10^4 cells/cm^2 [21,22]. To avoid frequent enzymatic treatment and to avoid contact deficiency, plating densities of $2-3 \times 10^3$ cells/cm^2 are recommended in the literature [23]. Based on this, we selected a plating density of 2.5×10^3 cells/cm^2. In contrast, the confluence for passaging/harvesting is stably described in protocols to be around 80% [15,19,40,43]. Based on local protocols, we used a harvesting/passaging confluence of >70%, to avoid contact inhibition of the highly proliferative hUC-MSCs and to obtain consistent growth results.

We used our standardized method to isolate and expand MSCs of 90 hUCs. The time from culture initiation to harvest at P0 was approximately 10 days and P1 population doubling showed a median of 21.6 hours. Others described a P0 duration of ~14 days [19,21] and a PDT varying between 24.8 and 29.4 hours using hPL [19,21] and 40.7 h using human serum as culture medium supplement [43], making our method considerably faster. This may be due to the relatively high amount of premature born donors and standardization of our protocol. The isolated hUC-MSC have a viability of >97% during P0 as well as P1, which is comparable or greater as compared with other studies [19,43]. For immunophenotypic characterization, we applied a method using standardized instruments settings, fluorochrome compensation and antibody staining ensuring comparability of all results [32]. We detected a purity of ~98.9% in P1 hUC-MSCs, which was consistent throughout all 90 hUC-MSC isolates and comparable or improved as compared with other studies [19,21,43], demonstrating reproducibility of our method.

Next to variable protocol and reagent selection, heterogenous donor characteristics, including sex, gestational age, mode of delivery and birth weight, introduce variability. Yet, we found that the variability in donor characteristics did not impact the characteristics of our hUC-MSC isolates. This is in line with a previous study that could not detect a difference in hUC-MSC isolation and characteristics between male and female donors [43], confirming the robustness of our culture method across donors. However, we found that a lower gestational age, a lower birth weight and the delivery by cesarean section were correlated with a decreased time to P0 harvest. This contrasts with a previous study reporting a decreased MSC isolation efficiency in MSCs derived from cesarean delivery as compared with vaginal birth [43]. We hypothesize that in our study the time to complete P0 is decreased, due to an increased migratory capacity of the MSCs obtained from donors born at an early gestational age. The correlations with mode of delivery and birthweight may be a secondary effect, deriving from the fact that pre-term neonates are lighter and more frequently born by Cesarean section.

UCs from different donors vary in features such as the amount of coiling and edematous Wharton's jelly, which can impact UC dissection and explants composition [48,49]. To our knowledge, we are the first to investigate the effect of various UC morphologies on the MSC isolation parameters, characteristics and population purity. We found no correlation between different UC phenotypes and characteristics of the hUC-MSC isolates, ensuring the robustness of our protocol across donors.

After demonstrating robustness of our method across donor and UC-types, we aimed to functionally characterize the generated hUC-MSC isolates. To that end, we differentiated MSCs obtained from three random UC donors towards adipocytes, osteoblasts and chondrocytes. We found a reduced capacity of hUC-MSCs to differentiate toward each of the lineages as compared with BM-MSCs, which differentiate efficiently into all three lineages. Previous studies describing the differentiation capacity of hUC-MSCs show mixed results. Although some describe hUC-MSCs to fail differentiation towards adipocytes, osteoblasts and chondrocytes [28], others report that UC-MSCs have the capacity to differentiate into all three lineages [44,50]. Yet, studies comparing hUC-MSC and BM-MSCs invariably report a reduced differentiation capacity of hUC-MSCs [21,29,30]. hUC-MSCs have been described to have greater expression levels of pluripotency markers such as Oct-3/4, Sox-2 and SSEA-4 as compared with BM-MSCs, indicating their less-mature character [12,51]. Therefore, it is possible that hUC-MSCs initiate differentiation when exposed to differentiation factors but do not readily proceed to full differentiation. In that case hUC-MSC may require tailored protocols to ensure a stable, reproducible, and complete differentiation towards adipocytes, osteoblasts and chondrocytes.

The ability to suppress T-cell proliferation makes hUC-MSCs a promising therapeutic agent and subject of numerous clinical trials [52]. By performing T-cell proliferation inhibition assays, we were able to demonstrate this immune-modulatory capacity of the hUC-MSCs. Therefore, our standardized method may also contribute to the standardization of hUC-MSC manufacturing methods.

Conclusions

We developed a standardized and robust method for the isolation and culture of hUC-MSCs. This protocol was shown to be stable across 90 hUC donors and hUC morphologies. After birth, a collection time of 6 h with an additional 48 h to process can be applied without impacting hUC-MSC characteristics. The removal of blood vessels before explant culture improves hUC-MSC purity of the hUC isolates. The culture in αMEM-hPL increases reproducibility, expansion rate and improves MSC characteristics as compared with DMEM-FBS. Our established protocol yields hUC-MSCs with a high purity, proliferative capacity, and viability. With this method, we have set the next step in unifying protocol choices regarding the isolation and culture of hUC-MSCs and thereby lay a foundation to advance the reliability and comparability of results obtained from hUC-MSCs of different donors.

Funding

This work is funded by an Established Investigator Grant from the Dutch Heart Foundation (2017T075) and by a grant (Grant for

Growth Innovation, GGI) from Merck Healthcare KgaA, Darmstadt, Germany. The funders had no role in study design, data collection, analysis, decision to publish or preparation of the manuscript.

Author Contributions

Conception and design of the study: MvP, BTH, PT, JMMK, AAWR, CdB, MCH, EL. Acquisition of data: PT, LAF, SGG, MvH. Analysis of the data: PT. Interpretation of data: PT, MvP, BTH, YFMR, LEM. All authors have contibuted to drafting and revising the manuscript and approved the final article.

Declaration of Competing Interest

The authors have no commercial, proprietary or financial interest in the products or companies described in this article.

Acknowledgments

The authors thank all mothers and fathers who participated in the Twinlife study with their newborn twins.

Supplementary materials

Supplementary material associated with this article can be found in the online version at doi:10.1016/j.jcyt.2023.07.004.

References

[1] Todtenhaupt P, van Pel M, Roest AAW, Heijmans BT. Mesenchymal stromal cells as a tool to unravel the developmental origins of disease. Trends Endocrinol Metab 2022;33:614–27.
[2] Han Y, Li X, Zhang Y, Han Y, Chang F, Ding J. Mesenchymal stem cells for regenerative medicine. Cells 2019;8:886.
[3] Pittenger MF, Discher DE, Péault BM, Phinney DG, Hare JM, Caplan AI. Mesenchymal stem cell perspective: cell biology to clinical progress. Npj Regen Med 2019;4:22.
[4] Weiss ARR, Dahlke MH. Immunomodulation by mesenchymal stem cells (MSCs): mechanisms of action of living, apoptotic, and dead MSCs. Front Immunol 2019;10:1191.
[5] Mebarki M, Abadie C, Larghero J, Cras A. Human umbilical cord-derived mesenchymal stem/stromal cells: a promising candidate for the development of advanced therapy medicinal products. Stem Cell Res Ther 2021;12:152.
[6] Friedenstein AJ, Chailakhyan RK, Latsinik NV, Panasyvk AF, Keiliss-Borok IV. Stromal cells responsible for transferring the microenvironment of the hemopoietic tissues: cloning in vitro and retransplantation in vivo. Transplantation 1974;17:331–40.
[7] Nombela-Arrieta C, Ritz J, Silberstein LE. The elusive nature and function of mesenchymal stem cells. Nat Rev Mol Cell Biol 2011;12:126–31.
[8] Wagner W, Ho AD. Mesenchymal stem cell preparations-comparing apples and oranges. Stem Cell Rev 2007;3:239–48.
[9] Hass R, Kasper C, Böhm S, Jacobs R. Different populations and sources of human mesenchymal stem cells (MSC): a comparison of adult and neonatal tissue-derived MSC. Cell Commun Signal 2011;9:12.
[10] Kong CM, Lin HD, Biswas A, Bongso A, Fong CY. Manufacturing of human Wharton's jelly stem cells for clinical use: selection of serum is important. Cytotherapy 2019;21:483–95.
[11] Kurogi H, Takijiri T, Sakumoto M, Isogai M, Takahashi A, Okubo T, et al. Study on the umbilical cord-mesenchymal stem cell manufacturing using clinical-grade culture medium. Tissue Eng Part C Methods 2022;28:23–33.
[12] Moretti P, Hatlapatka T, Marten D, Lavrentieva A, Majore I, Hass R, et al. Mesenchymal stromal cells derived from human umbilical cord tissues: primitive cells with potential for clinical and tissue engineering applications. Adv Biochem Eng Biotechnol, 123; 2010. p. 201029–54.
[13] Li DR, Cai JH. Methods of isolation, expansion, differentiating induction and preservation of human umbilical cord mesenchymal stem cells. Chin Med J (Engl) 2012;125:4505–10.
[14] Chatzistamatiou TK, Papassavas AC, Michalopoulos E, Gamaloutsos C, Mallis P, Gontika I, et al. Optimizing isolation culture and freezing methods to preserve Wharton's jelly's mesenchymal stem cell (MSC) properties: an MSC banking protocol validation for the Hellenic Cord Blood Bank. Transfusion 2014;54:3108–20.
[15] Salehinejad P, Banu Alitheen N, Ali AM, Omar AR, Mohit M, Janzamin E, et al. Comparison of different methods for the isolation of mesenchymal stem cells from human umbilical cord Wharton's jelly. In Vitro Cell Dev Biol Anim 2012;48:75–83.
[16] Yoon JH, Roh EY, Shin S, Jung NH, Song EY, Chang JY, et al. Comparison of explant-derived and enzymatic digestion-derived MSCs and the growth factors from Wharton's jelly. Biomed Res Int 2013;2013:1–8.
[17] Zheng S, Gao Y, Chen K, Liu Y, Xia N, Fang F. A Robust and highly efficient approach for isolation of mesenchymal stem cells from Wharton's jelly for tissue repair. Cell Transplant 2022;31:096368972210843.
[18] De Bruyn C, Najar M, Raicevic G, Meuleman N, Pieters K, Stamatopoulos B, et al. A rapid, simple, and reproducible method for the isolation of mesenchymal stromal cells from Wharton's jelly without enzymatic treatment. Stem Cells Dev 2011;20:547–57.
[19] Majore I, Moretti P, Stahl F, Hass R, Kasper C. Growth and differentiation properties of mesenchymal stromal cell populations derived from whole human umbilical cord. Stem Cell Rev Reports 2011;7:17–31.
[20] Badraiq H, Devito L, Ilic D. Isolation and expansion of mesenchymal stromal/stem cells from umbilical cord under chemically defined conditions, 2014, p. 65–71. https://doi.org/10.1007/7651_2014_116.
[21] Capelli C, Gotti E, Morigi M, Rota C, Weng L, Dazzi F, et al. Minimally manipulated whole human umbilical cord is a rich source of clinical-grade human mesenchymal stromal cells expanded in human platelet lysate. Cytotherapy 2011;13:786–801.
[22] Lu LL, Liu YJ, Yang SG, Zhao QJ, Wang X, Gong W, et al. Isolation and characterization of human umbilical cord mesenchymal stem cells with hematopoiesis-supportive function and other potentials. Haematologica 2006;91:1017–26.
[23] Hoffmann A, Floerkemeier T, Melzer C, Hass R. Comparison of in vitro-cultivation of human mesenchymal stroma/stem cells derived from bone marrow and umbilical cord. J Tissue Eng Regen Med 2017;11:2565–81.
[24] Viswanathan S, Shi Y, Galipeau J, Krampera M, Leblanc K, Martin I, et al. Mesenchymal stem versus stromal cells: International Society for Cell & Gene Therapy (ISCT®) Mesenchymal Stromal Cell committee position statement on nomenclature. Cytotherapy 2019;21:1019–24.
[25] Dominici M, Le Blanc K, Mueller I, Slaper-Cortenbach I, Marini FC, Krause DS, et al. Minimal criteria for defining multipotent mesenchymal stromal cells. The International Society for Cellular Therapy position statement. Cytotherapy 2006;8:315–7.
[26] Phinney DG, Galipeau J. Manufacturing mesenchymal stromal cells for clinical applications: a survey of Good Manufacturing Practices at U.S. academic centers. Cytotherapy 2019;21:782–92.
[27] Trento C, Bernardo ME, Nagler A, Kuçi S, Bornhäuser M, Köhl U, et al. Manufacturing mesenchymal stromal cells for the treatment of graft-versus-host disease: a survey among centers affiliated with the European Society for Blood and Marrow Transplantation. Biol Blood Marrow Transplant 2018;24:2365–70.
[28] Bosch J, Houben AP, Radke TF, Stapelkamp D, Bünemann E, Balan P, et al. Distinct differentiation potential of "MSC" derived from cord blood and umbilical cord: are cord-derived cells true mesenchymal stromal cells? Stem Cells Dev 2012;21:1977–88.
[29] van der Garde M, van Pel M, Millán Rivero JE, de Graaf-Dijkstra A, Slot MC, Kleinveld Y, et al. Direct comparison of Wharton's jelly and bone marrow-derived mesenchymal stromal cells to enhance engraftment of cord blood $CD34^+$ transplants. Stem Cells Dev 2015;24:2649–59.
[30] Kwon A, Kim Y, Kim M, Kim J, Choi H, Jekarl DW, et al. Tissue-specific differentiation potency of mesenchymal stromal cells from perinatal tissues. Sci Rep 2016;6:23544.
[31] Groene SG, Todtenhaupt P, Van Zwet EW, Van Pel M, Berkhout RJM, Haak MC, et al. TwinLIFE: the Twin Longitudinal Investigation of FEtal Discordance. Twin Res Hum Genet 2019;22:617–22.
[32] Kalina T, Flores-Montero J, van der Velden VHJ, Martin-Ayuso M, Böttcher S, Ritgen M, et al. EuroFlow standardization of flow cytometer instrument settings and immunophenotyping protocols. Leukemia 2012;26:1986–2010.
[33] Melief SM, Zwaginga JJ, Fibbe WE, Roelofs H. Adipose tissue-derived multipotent stromal cells have a higher immunomodulatory capacity than their bone marrow-derived counterparts. Stem Cells Transl Med 2013;2:455–63.
[34] Bomer N, den Hollander W, Ramos YFM, Bos SD, van der Breggen R, Lakenberg N, et al. Underlying molecular mechanisms of DIO2 susceptibility in symptomatic osteoarthritis. Ann Rheum Dis 2015;74:1571–9.
[35] Astori G, Amati E, Bambi F, Bernardi M, Chieregato K, Schäfer R, et al. Platelet lysate as a substitute for animal serum for the ex-vivo expansion of mesenchymal stem/stromal cells: present and future. Stem Cell Res Ther 2016;7:93.
[36] Palombella S, Perucca Orfei C, Castellini G, Gianola S, Lopa S, Mastrogiacomo M, et al. Systematic review and meta-analysis on the use of human platelet lysate for mesenchymal stem cell cultures: comparison with fetal bovine serum and considerations on the production protocol. Stem Cell Res Ther 2022;13:142.
[37] Mendicino M, Bailey AM, Wonnacott K, Puri RK, Bauer SR. MSC-based product characterization for clinical trials: an FDA perspective. Cell Stem Cell 2014;14:141–5.
[38] Dong-rui LI, Jian-hui C. Methods of isolation, expansion, differentiating induction and preservation of human umbilical cord mesenchymal stem cells. Chin Med J (Engl) 2012;125:4504–10.
[39] Pereira WC, Khushnooma I, Madkaikar M, Ghosh K. Reproducible methodology for the isolation of mesenchymal stem cells from human umbilical cord and its potential for cardiomyocyte generation. J Tissue Eng Regen Med 2008;2:394–9.
[40] Petsa A, Gargani S, Felesakis A, Grigoriadis N, Grigoriadis I. Effectiveness of protocol for the isolation of Wharton's jelly stem cells in large-scale applications. In Vitro Cell Dev Biol Anim 2009;45:573–6.
[41] Han YF, Tao R, Sun TJ, Chai JK, Xu G, Liu J. Optimization of human umbilical cord mesenchymal stem cell isolation and culture methods. Cytotechnology 2013;65:819–27.
[42] Yi X, Chen F, Liu F, Peng Q, Li Y, Li S, et al. Comparative separation methods and biological characteristics of human placental and umbilical cord mesenchymal stem cells in serum-free culture conditions. Stem Cell Res Ther 2020;11:183.

[43] Smith JR, Pfeifer K, Petry F, Powell N, Delzeit J, Weiss ML. Standardizing umbilical cord mesenchymal stromal cells for translation to clinical use: selection of GMP-compliant medium and a simplified isolation method. Stem Cells Int 2016;2016:1–16.
[44] Skiles ML, Marzan AJ, Brown KS, Shamonki JM. Comparison of umbilical cord tissue-derived mesenchymal stromal cells isolated from cryopreserved material and extracted by explantation and digestion methods utilizing a split manufacturing model. Cytotherapy 2020;22:581–91.
[45] Bourin P, Gadelorge M, Peyrafitte J-A, Fleury-Cappellesso S, Gomez M, Rage C, et al. Mesenchymal progenitor cells: tissue origin, isolation and culture. Transfus Med Hemotherapy 2008;35:160–7.
[46] Bui HTH, Nguyen LT, Than UTT. Influences of xeno-free media on mesenchymal stem cell expansion for clinical application. Tissue Eng Regen Med 2021;18:15–23.
[47] Alonso-Camino V, Mirsch B. Rapid expansion of mesenchymal stem/stromal cells using optimized media supplemented with human platelet lysate PLTMax® or PLTGold®, suitable for cGMP expansion at large scale. Cytotherapy 2019;21:S85.
[48] Baergen RN. Manual of pathology of the human placenta. Boston, MA: Springer US; 2011.
[49] Stanek J. Association of coexisting morphological umbilical cord abnormality and clinical cord compromise with hypoxic and thrombotic placental histology. Virchows Arch 2016;468:723–32.
[50] Kong C-M, Subramanian A, Biswas A, Stunkel W, Chong Y-S, Bongso A, et al. Changes in stemness properties, differentiation potential, oxidative stress, senescence and mitochondrial function in Wharton's jelly stem cells of umbilical cords of mothers with gestational diabetes mellitus. Stem Cell Rev Reports 2019;15:415–26.
[51] Jo CH, Kim O-S, Park E-Y, Kim BJ, Lee J-H, Kang S-B, et al. Fetal mesenchymal stem cells derived from human umbilical cord sustain primitive characteristics during extensive expansion. Cell Tissue Res 2008;334:423–33.
[52] Cutler AJ, Limbani V, Girdlestone J, Navarrete CV. Umbilical cord-derived mesenchymal stromal cells modulate monocyte function to suppress T cell proliferation. J Immunol 2010;185:6617–23.